

# FABRICATION AND TEST OF A 1 M LONG SINGLE-APERTURE 11 T Nb<sub>3</sub>SN DIPOLE FOR LHC UPGRADES\*

A.V. Zlobin<sup>#</sup>, N. Andreev, G. Apollinari, E. Barzi, R. Bossert, G. Chlachidze, J. DiMarco,  
F. Nobrega, I. Novitski, D. Turrioni, G. Velez, FNAL, Batavia, IL 60510, U.S.A.

B. Auchmann, M. Karppinen, L. Rossi, D. Smekens, CERN, CH-1211 Geneva 23, Switzerland

## Abstract

FNAL and CERN are carrying out a joint R&D program with the goal of building a 5.5-m long twin-aperture Nb<sub>3</sub>Sn dipole prototype suitable for installation in the LHC. An important part of the program is the development and test of a series of short single-aperture demonstration dipoles with a nominal field of 11 T at the LHC nominal current of 11.85 kA and 20% margin. This paper describes design features and test results of a 1 m long single-aperture Nb<sub>3</sub>Sn demonstrator dipole.

## INTRODUCTION

The LHC operation plans include an upgrade of the LHC collimation system [1]. Additional collimators will be installed in the dispersion suppression (DS) regions around points 2, 3 and 7, and high luminosity interaction regions at points 1 and 5. The ~3.5 m space required for the additional collimators could be provided by using 11 T Nb<sub>3</sub>Sn dipoles as replacements for several 8.33 T LHC main NbTi dipoles (called MB), which deliver the same integrated strength at the nominal LHC current as MB dipoles.

To demonstrate feasibility, CERN and FNAL have started in October 2010 an R&D program to build by 2015 a 5.5 m long twin-aperture Nb<sub>3</sub>Sn dipole for the LHC upgrade. Two such cold masses with a collimator in between will replace one 14.3 m long MB dipole. The program started with the design and construction of a 2 m long single-aperture Nb<sub>3</sub>Sn demonstrator magnet [2] which was tested at FNAL in June 2012 and reached 10.4 T at the LHC operating temperature of 1.9 K [3]. To improve the magnet quench performance and field quality, as well as to demonstrate performance reproducibility, the fabrication of four 1 m long collared coils was started at FNAL last year. These collared coils will be tested first in a single-aperture configuration and then assembled and tested inside a common iron yoke (twin-aperture configuration). In parallel, two 2 m long twin-aperture demonstrator dipole magnets will be built at CERN to optimize the quench performance, field quality and quench protection of Nb<sub>3</sub>Sn coils and a somewhat different mechanical concept of the collar and yoke [4].

This paper describes the design features and test results of the first 1 m long single-aperture Nb<sub>3</sub>Sn dipole fabricated and tested recently at FNAL.

\* Work supported by Fermi Research Alliance, LLC, under contract No. DE-AC02-07CH11359 with the U.S. Department of Energy and European Commission under FP7 project HiLumi LHC, GA no.284404  
<sup>#</sup> zlobin@fnal.gov

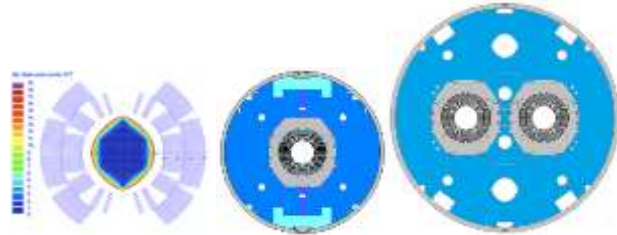


Figure 1: The 2-layer coil (left), single-aperture (middle) and twin-aperture (right) dipole cold masses. The dark area in the coil bore corresponds to relative field errors below  $10^{-4}$ .

## DIPOLE DESIGN AND PARAMETERS

The design concepts of 11 T Nb<sub>3</sub>Sn dipole in single-aperture and twin-aperture configurations are described in [3, 4]. The magnet coil was optimized to provide a dipole field above 11 T in a 60 mm aperture at the 11.85 kA current with 20% margin, and geometrical field errors below  $10^{-4}$ . Fig. 1 (left) shows the optimized 6-block coil of the demonstrator dipole with relative geometrical field errors in the aperture (dark area). The cross-sections of the single- and twin-aperture cold masses of 11 T dipole (FNAL design) are also shown in Fig. 1 (middle and right).

The design of the dipole mechanical structure and the coil pre-stress were optimized to maintain the coils under compression up to the ultimate design field of 12 T and keep the coil maximum stress below the safe level of 165 MPa during magnet assembly and operation [2].

The calculated design parameters of the 2 m long single- and twin-aperture dipole magnets at  $I_{nom}$  of 11.85 kA,  $T_{op}$  of 1.9 K, nominal strand  $J_c(12T, 4.2K)$  of 2750 A/mm<sup>2</sup> and cable  $I_c$  degradation of 10% are shown in Table 1. For a 1 m long model in the single-aperture configuration, the calculated nominal parameters are slightly higher (for example, the central field is 11.07 T at  $I_{nom}=11.85$  kA) due to field enhancement in the magnet central cross-section from the coil ends.

Table 1: 2 m long Dipole Parameters at  $I_{nom}=11.85$  kA.

Parameter	Single-aperture	Twin-aperture
Yoke outer diameter, mm	400	550
Nominal bore field at $I_{nom}$ , T	10.88	11.23
Short sample field $B_{SSL}$ at $T_{op}$ , T	13.4	13.9
Margin $B_{nom}/B_{SSL}$ at $T_{op}$ , %	81	83
Stored energy at $I_{nom}$ , kJ/m	424	969
$F_x$ /quadrant at $I_{nom}$ , MN/m	2.89	3.16
$F_y$ /quadrant at $I_{nom}$ , MN/m	-1.58	-1.59

## MODEL CONSTRUCTION

The magnet coils were made of Rutherford cable [3] with 40 Nb<sub>3</sub>Sn strands, a 15 degree transposition angle, and 0.025 mm thick and 11 mm wide stainless steel core. Cable packing factor is 88%. The cable uses 0.7 mm Nb<sub>3</sub>Sn RRP-150/169 strand [5]. The strand cross-section and a picture of the cored cable are shown in Fig. 2.



Figure 2: RRP-150/169 strand and 40-strand cable with a SS core.

Each coil consists of 2 layers and 56 turns. Both layers were wound from a single ~100 m long piece of cable wrapped with 0.075 mm thick and 12.7 mm wide E-glass tape with ~50% overlap. The coil poles were made of Ti alloy, and wedges and end spacers were made of stainless steel. The coil fabrication process is based on the wind-and-react method. During winding each coil layer was filled with CTD-1202X liquid ceramic binder and cured under a small pressure at 150°C for 0.5 hour. During curing the coil layers were shimmed azimuthally to a size 1-1.5 mm smaller than the nominal coil size to provide room for the Nb<sub>3</sub>Sn cable to expand during reaction. Each coil was reacted in Argon using a 3-step cycle with  $T_{max}=665^{\circ}C$  for 50 hours. Coils were impregnated with CTD101K epoxy and cured at 125°C for 21 hours.

Two coils (#5 and #7) surrounded by the ground insulation and stainless steel protection shells were placed inside laminated stainless steel collars. The coil ground insulation consists of 1 layer of 0.114 mm Kapton film with adhesive and 4 layers of 0.125 mm thick Kapton film. Two quench protection heaters composed of 0.025 mm thick stainless steel strips were mounted on each side of the coil between the 1<sup>st</sup> and 2<sup>nd</sup> Kapton layers of the ground insulation. The strips on each side of each coil were connected in series forming two heater circuits.

The collared coil was installed inside a vertically split iron yoke with a 400 mm outer diameter and fixed with Al clamps. The yoke length covers the entire coil and the Nb<sub>3</sub>Sn/NbTi lead splices. The 12 mm thick bolted skin made of stainless steel provides the coil final pre-compression. Two 50 mm thick stainless steel end plates bolted to the shell restrict the axial coil motion. A picture of a 1 m long single-aperture cold mass is shown Fig. 3.



Figure 3: The 1 m long coil (left) and the single-aperture dipole cold mass MBHSP02 (right).

## TEST RESULTS

The 1 m long dipole model (MBHSP02) was tested at the FNAL Vertical Magnet Test Facility in March 2013.

The quench current limits for the dipole model, estimated based on measured witness sample data, are 13.8 kA (15.4 kA) at 4.5 K (1.9 K), which corresponds to bore fields of 12.7 T (14.1 T) respectively. Note that the ultimate design field for this magnet is 12 T; it is limited by the maximum safe coil pre-stress level.

The training quenches are shown in Fig. 4. Training started at 4.5 K with a current ramp rate of 20 A/s. The first quench at 9.57 kA corresponds to 72% of the short sample limit (SSL) at 4.5 K. After 17 quenches in the inner-layer end blocks of both coils, a few quenches were detected in the outer mid-plane blocks of coil #7 (red markers in Fig. 4).

The magnet training was then continued at 1.9 K. The field of 11 T was reached after 30 training quenches. The maximum bore field in the magnet is 11.7 T or 97.5% of the magnet design field. All quenches at 1.9 K also occurred in the inner-layer end blocks of both coils. A few quenches at 4.5 K and 1.9 K, after magnet training at 1.9 K, illustrate the magnet training memory (Fig. 4).

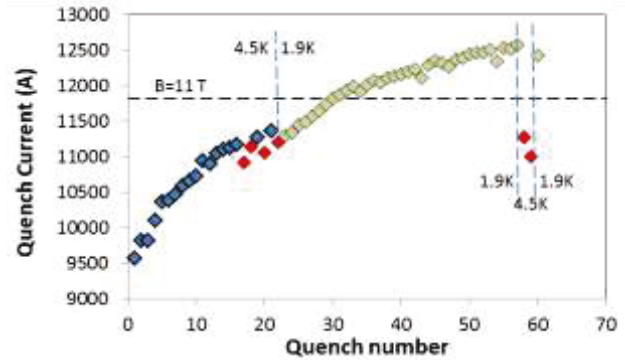


Figure 4: Magnet training.

Magnet current was ramped at 10-20 A/s to a pre-set current below its quench value and held until quench. Fig. 5 shows the holding time to quench vs. current at 4.5 K and 1.9 K. Data with “0” holding time represents the regular quenches at  $dI/dt=20$  A/s. All the holding quenches (except for those with “0” holding time) were initiated in the outer-layer mid-plane block of coil #7.

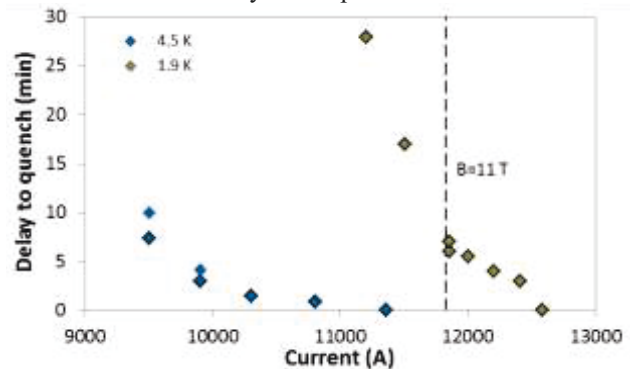


Figure 5: Holding time to quench vs. plateau current.

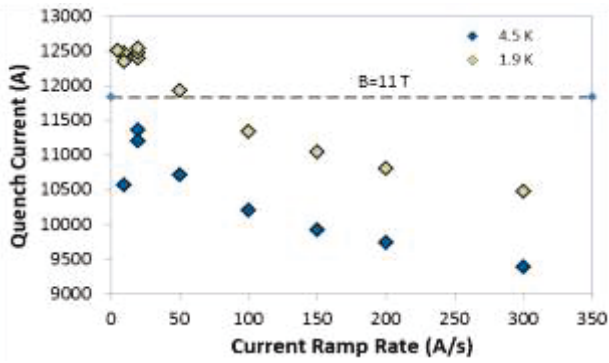


Figure 6: Ramp rate sensitivity of magnet quench current.

Ramp rate dependences of the magnet quench current are shown in Fig. 6. The stainless steel core used in this model suppressed cable eddy currents and reduced the magnet ramp rate sensitivity. Extrapolation of the quench currents to  $dI/dt=0$  gives the  $I_{\max}(4.5K)\sim 12$  kA and  $I_{\max}(1.9K)\sim 13.5$  T that is noticeably lower than the SSL.

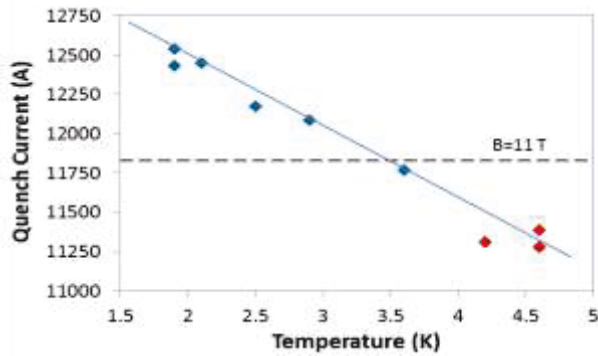


Figure 7: Temperature dependence of quench current.

The temperature dependence of the quench current measured at a ramp rate of 20 A/s is shown in Fig. 7. The magnet demonstrates the regular temperature dependence of quench current. All quenches at intermediate temperatures below 4 K were initiated in the coil inner-layer end blocks. The quenches marked in red color started in the outer-layer midplane block of coil #7.

Magnetic measurements were done using a 130 mm long 16-layer Printed Circuit Board (PCB) probe [6]. Transfer function ( $TF$ ) and sextupole ( $b_3$ ) loops vs. current with ramp rates of 10-80 A/s at 1.9 K are shown in Figs. 8-9. The large persistent current effect, seen at

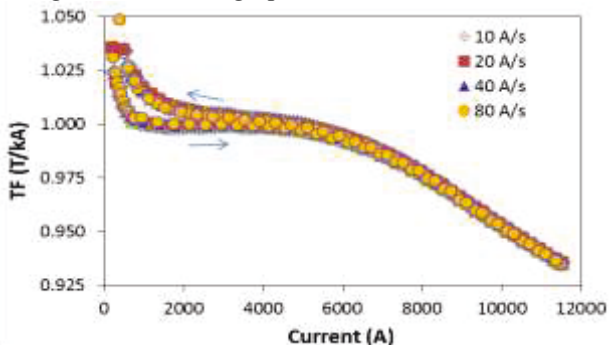


Figure 8: Transfer function  $TF$  vs. magnet current.

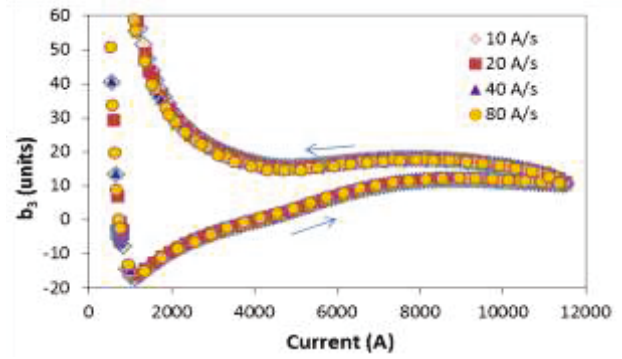


Figure 9: Sextupole  $b_3$  vs. magnet current.

low currents in the  $TF$  and  $b_3$ , is due to large  $D_{eff}$  and  $J_c$  of the used  $Nb_3Sn$  strand. The ramp rate effect is small as expected for the cored cable. The iron saturation in  $TF$  and  $b_3$  starts, as predicted, at currents above 4 kA. The unexpectedly large ( $\sim 7$  units)  $b_3$  decay effect at  $I_{inj}=760$  A in this model was not seen in the 2 m long magnet [7].

Table 2: Field harmonics at  $I=3.5$  kA.

$n$	2	3	4	5	6	7	9
$a_n$	0.14	-1.44	0.24	0.15	0.00	-0.05	0.12
$b_n$	-4.93	8.44	-0.17	1.02	-0.23	0.03	0.18

Table 2 presents the geometrical harmonics averaged over the probe length at 3.5 kA. Significant improvement of geometrical harmonics was achieved in this magnet with respect to the 2 m long demonstrator [7]. Still large values of  $b_3$  and  $a_3$  are likely due to the coil shimming used to achieve the required coil prestress, and large  $b_2$  is due to the coil azimuthal misalignment inside the collar. Both effects will be minimized in the next models.

## CONCLUSION

The 1<sup>st</sup> of four 1 m long collared coils to be used in the twin-aperture  $Nb_3Sn$  dipole models has been built and tested at FNAL in a single-aperture configuration. The magnet reached 11.7 T at 1.9 K or 97.5% of its design field and demonstrated improved geometrical harmonics and eddy current effect. Yet, large quench current degradation, quenching at a current plateau, and large  $b_3$  decay were observed. The causes of that are being studied. New coils for the 2<sup>nd</sup> aperture are being made.

## REFERENCES

- [1] L. Bottura et al., *IEEE Trans. on Applied Supercond.*, Vol. 22, N 3, 2012, p. 4002008.
- [2] A.V. Zlobin et al., *PAC'2011*, NYC, 2011, p. 1460.
- [3] A.V. Zlobin et al., *IEEE Trans. on Appl. Supercond.*, Vol. 23, N 3, 2013, p. 4000904.
- [4] M. Karppinen et al., *IEEE Trans. on Appl. Supercond.*, Vol. 22, N 3, 2012, p. 4901504.
- [5] E. Barzi et al., *IEEE Trans. on Appl. Supercond.*, Vol. 22, N 3, 2012, p. 6001405.
- [6] J. DiMarco et al., *FERMILAB-CONF-12-570-TD*.
- [7] N. Andreev et al., *IEEE Trans. on Appl. Supercond.*, Vol. 23, N 3, 2013, p. 4001804.